

# METASTABLE CRYSTAL STRUCTURES OF SOLID HYDROGEN

*G. W. Collins*

*W. G. Unites*

*E. R. Mapoles*

*T. P. Bernat*

---

---

## Introduction

All current ignition target designs for inertial confinement fusion (ICF) require a uniform cryogenic (liquid or solid) deuterium–tritium (DT) fuel layer. However, it is difficult to support a uniform liquid DT layer inside a capsule in the presence of gravity.<sup>1</sup> Fortunately, a solid DT layer is stable in the presence of gravity and self-symmetrizes due to the natural heating from tritium beta decay (beta-layering).<sup>2</sup> Recent experiments show that beta layering can produce a surface roughness of 1  $\mu\text{m}$  rms, which is smooth enough for current National Ignition Facility ignition target designs. The surface roughness of these polycrystalline DT layers is determined by the way crystal facets stack up to conform to the 1-mm radius of curvature. If we could produce a stable amorphous DT layer, the surface roughness could be reduced significantly. Alexandrova et al. claim to have observed such an amorphous layer of  $\text{H}_2$ .<sup>3</sup> In this article, we describe the equilibrium and metastable structures of solid hydrogen. Since the crystal structure of all the hydrogen isotopes is the same, we work with  $\text{H}_2$  and  $\text{D}_2$  instead of DT.

We begin by reviewing some basic properties of solid hydrogen. Because the interaction between hydrogen molecules is weak, the rotational quantum number is well defined in the low-pressure solid at temperatures above  $0.2T_{\text{tp}}$ , and most of the molecules are either in the ground ( $J=0$ ) or first excited ( $J=1$ ) rotational state.  $T_{\text{tp}}$  is the triple-point temperature for a particular hydrogen isotope or mixture:  $T_{\text{tp}}(J=0 \text{ H}_2) = 13.8 \text{ K}$  and  $T_{\text{tp}}(J=0 \text{ D}_2) = 18.7 \text{ K}$ .<sup>4</sup> All the hydrogens typically form an hcp structure near their respective  $T_{\text{tp}}$ .<sup>5,6</sup> However, at low enough temperature and large  $J=1$  concentration ( $[J=1] > 55\%$ ), the lattice transforms to fcc with the molecules oriented. This phase transition lowers the electric quadrupole–quadrupole energy for  $J=1$  molecules by about 5 K/molecule, which is much

greater than the  $\sim 1 \text{ mK}$ /molecule energy difference between disordered hcp and fcc structures. In  $J=0$  hydrogen, the free energy difference between hcp and fcc is not well understood, but the equilibrium crystal structure at all temperatures and pressures below  $\sim 100 \text{ GPa}$  is hcp.<sup>7</sup>

Rare gas solids also form simple molecular solids with lattice potentials similar to hydrogen. However, Ne, Ar, Kr, and Xe crystallize into fcc at low pressure, while the lightest rare gas,  $^4\text{He}$ , primarily forms an hcp structure at low temperature and pressure, and fcc only at high temperature and pressure. The hcp structure forms in low pressure  $^4\text{He}$  and possibly  $J=0$  hydrogen because the dispersion interaction for the closed shell  $S$  state orbital is comparatively small.<sup>8</sup>

While hcp is the equilibrium structure at low  $J=1$  concentrations, nonequilibrium hydrogen fcc structures have been observed.<sup>9</sup> In this article, we describe the temperature dependence and crystal morphology of metastable phases of  $J=0 \text{ H}_2$  and  $\text{D}_2$ .<sup>10</sup> We also show that (1) the metastable fcc phase is separated from hcp by a spectrum of energy barriers, (2) the fcc phase is less stable in  $\text{H}_2$  than in  $\text{D}_2$ , (3) the structural symmetry decreases as the deposition temperature  $T_{\text{d}}$  decreases, and (4) the crystallite length scale decreases with decreasing  $T_{\text{d}}$ . However, we find no evidence that an amorphous phase of hydrogen can be produced at temperatures as low as  $0.18T_{\text{tp}}$ .

To determine lattice structure, we detect the  $J=0 \rightarrow 2$  signal of the rotational Raman spectrum. In pure  $J=0$  solids, this signal produces a multiplet that can be a unique signature of the crystal lattice. A triplet is unique to hcp, whereas fcc symmetry produces a doublet. Van Kranendonk<sup>7</sup> outlines the calculational procedure for determining the spectral positions and intensity ratios. Some of our observations may be related to those of Silvera and Wijngaarden<sup>11</sup> and Durana and McTague,<sup>12</sup> who observed a four-peak

spectrum in rapidly pressurized hydrogen. Four peaks are expected if the Raman signal results from both hcp and fcc crystals because the high-energy shifted peaks for both hcp and fcc are close together and the low-energy shifted fcc signal is at lower energy than the other hcp lines.

## Experimental Details

For these experiments, a Cu sample cell is fitted with two opposing vertical  $\text{MgF}_2$ -coated sapphire windows that serve as the hydrogen substrate and permit optical access. The cell is connected to the cold tip of a He flow cryostat. Both a 30-K radiation shield and the outer vacuum jacket contain sapphire windows for optical access. A calibrated germanium resistance thermometer (GRT) is fitted on the Cu sample cell and checked against  $T_{\text{tp}}$  of  $\text{D}_2$  and  $\text{H}_2$ . At  $T > 0.5 T_{\text{tp}}$ , we compare the thermometer temperature with the temperature calculated from the hydrogen vapor pressure,<sup>13</sup> as measured by a capacitance manometer. The agreement between the vapor pressure and the GRT shows the accuracy of the temperature measurement to be better than 0.05 K.

The  $\text{H}_2$  and  $\text{D}_2$  gas were high-purity research grade, with an isotopic purity of 99.9% and 99.8% respectively. The samples studied contained a  $J=1$  concentration less than ~1%. The rotational and isotopic concentrations are determined by comparing the Raman line intensities for the  $J=0 \rightarrow 2$  and  $J=1 \rightarrow 3$  transitions. The hydrogen gas was cooled to ~20–30 K just before deposition. The deposition rates are determined from the layer thickness, measured by interferometry, vs time. All the samples were between 30 and 300  $\mu\text{m}$  thick.

We measured the Raman shift of the 488-nm line of an Ar ion laser in a back scattering geometry with a modified 0.5-m SPEX 1870 spectrograph fitted with a liquid-nitrogen-cooled CCD having a 22.5- $\mu\text{m}$  pixel width. We used  $f/3$  optics to couple light in and out of the sample. Our spectral resolution was ~0.4  $\text{cm}^{-1}$ . Line positions were determined from both a calibrated Th lamp and the triplet structure of  $\text{H}_2$  or  $\text{D}_2$  crystallized through the triple point, with their line positions as measured by Bhatnagar et al.<sup>14</sup> The laser power level (~1 to 100 mW in ~40  $\mu\text{m}^2$ ) did not influence the lattice structure or visually change the layer morphology.

## Raman Data

Figure 1 shows several different Raman spectra for vapor-deposited  $\text{H}_2$  or  $\text{D}_2$  layers. The spectra on the left and right are from  $\text{H}_2$  and  $\text{D}_2$  respectively. The three-peak spectrum in Fig. 1(a) is typical of  $\text{H}_2$  or  $\text{D}_2$  at  $T_{\text{d}} > 0.3 T_{\text{tp}}$ . The four-peak spectra in Fig. 1(b) and 1(e) are typical of  $3.5 \text{ K} \leq T_{\text{d}}(\text{H}_2) < 4 \text{ K}$  and  $4 \text{ K} < T_{\text{d}}(\text{D}_2)$

$\leq 6 \text{ K}$ , and of deposition rates of  $0.1 < R (\mu\text{m}/\text{min}) < 40$ . Figure 1(d) is typical for  $3.5 \leq T_{\text{d}}(\text{D}_2) < 4 \text{ K}$ , where it appears that the peaks in Fig. 1(e) shift toward an unresolved lineshape with two main branches. Figures 1(c) and 1(f) show the signals several minutes after rapidly warming  $\text{H}_2$  and  $\text{D}_2$  respectively. The quadruplet in Fig. 1(b) and 1(e) and the unresolved “doublet” in Fig. 1(d) transform to a triplet within minutes upon warming the sample rapidly through  $\sim 0.5 T_{\text{tp}}$ . At constant temperature the Raman spectra in Fig. 1 are stable for at least two days, the maximum duration of observation. Figure 2(a) shows the temperature dependence of the Raman spectrum of  $\text{D}_2$  for  $T_{\text{d}} = 5.3 \text{ K}$ . The steady decrease in the relative intensity of the first and fourth peaks with increasing temperature is not reversible upon cooling. There is a slight shift in the spectrum of  $\sim -0.45 \text{ cm}^{-1}$  upon warming from 5 to 7 K. The high-energy peak is shifted slightly more ( $\sim -0.70$  to  $-0.90 \text{ cm}^{-1}$ ) than the other, low-energy peaks. The quadruplet signal in  $\text{H}_2$  also transforms to a triplet upon slowly raising  $T$  to  $\sim 5.5 \text{ K}$ .

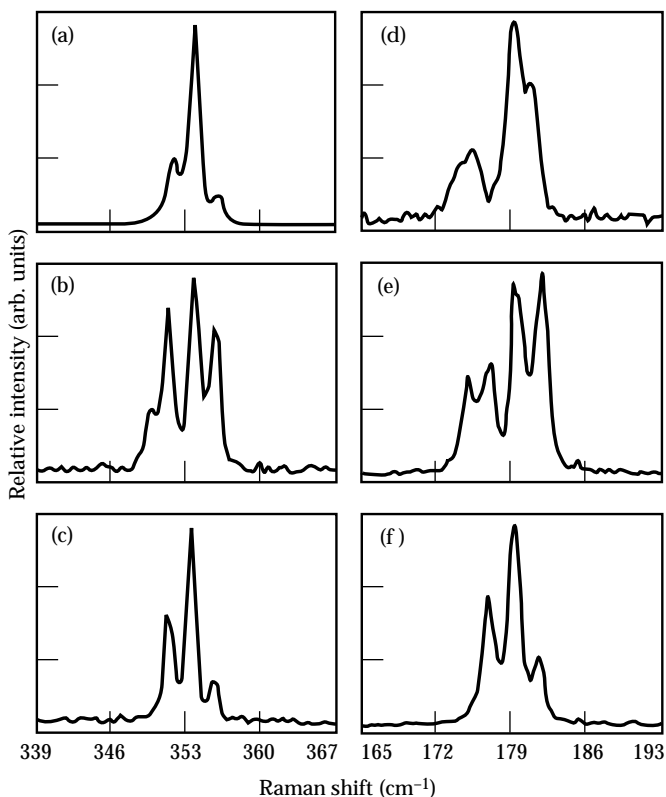


FIGURE 1.  $J=0 \rightarrow 2$  Raman signal for (a)  $\text{H}_2$  deposited at 5.5 K and 5  $\mu\text{m}/\text{min}$ , (b)  $\text{H}_2$  deposited at 3.5 K and 2  $\mu\text{m}/\text{min}$ , (c) same sample as Fig. 1(b) after warming from 3.5 K to 7 K, (d)  $\text{D}_2$  deposited at 3.5 K and 0.2  $\mu\text{m}/\text{min}$ , (e)  $\text{D}_2$  deposited at 5.2 K and 0.4  $\mu\text{m}/\text{min}$ , (f) same sample as Fig. 1(e) after warming from 5.2 K to 11.4 K. (10-06-0296-0312pb01)

In Fig. 2(b) we plot the intensity ratio of the low-energy Raman peak of the quadruplet divided by the average of the other three peaks,  $R_{\text{fcc/hcp}}$ , vs temperature (all values, not just the steady state value) from two different experiments. The large scatter of points at each

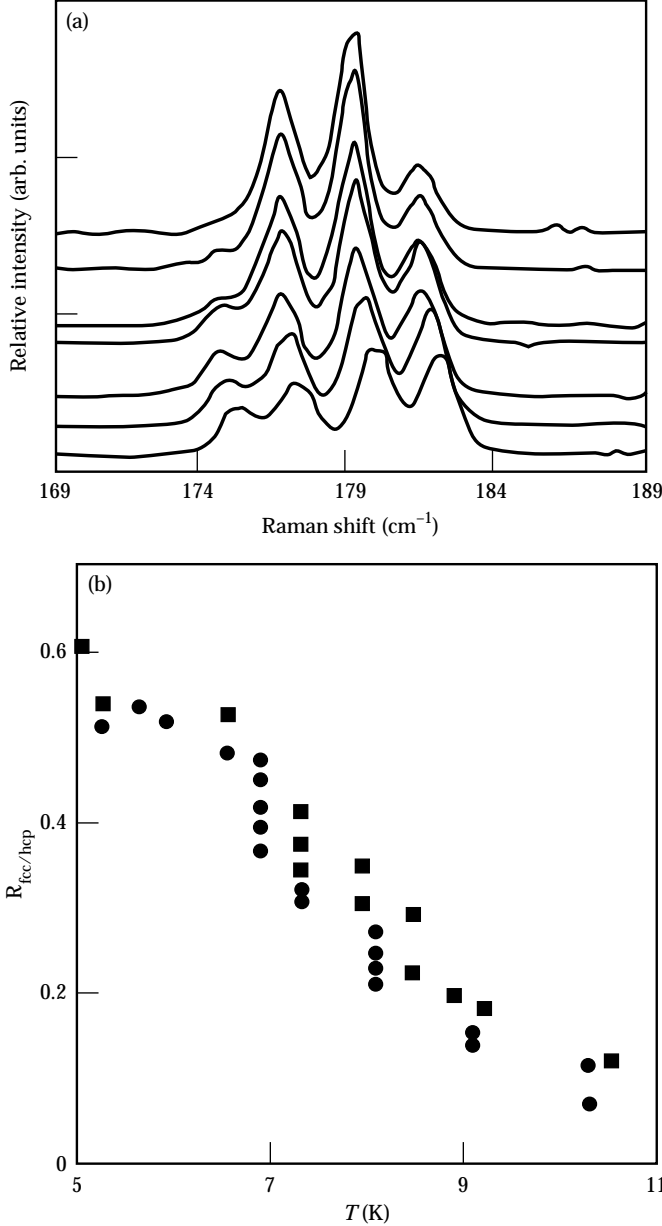


FIGURE 2. Temperature and time dependence of the  $J=0 \rightarrow 2$  Raman spectrum, upon warming solid  $J=0$   $D_2$ . (a)  $D_2$  deposited at 5.3 K and  $2.2 \mu\text{m}/\text{min}$  (from bottom to top) (i) after deposition at 5.3 K, (ii) after raising  $T$  to 6.9 K, (iii) after waiting at 6.9 K for 34 min, (iv) after raising  $T$  to 7.4 K and waiting 8 min, (v) after 13 min at 8.1 K, (vi) after 5 min at 9.1 K, and (vii) after 2 min at 10.4 K. (b) The low-energy Raman peak divided by the average of the other three peaks ( $R_{\text{fcc/hcp}}$ ) vs  $T$  from two different experiments. The circles show the same experiment as in Fig. 2(a). The squares show a similar experiment with  $J=0$   $D_2$  deposited at 5.1 K and  $0.4 \mu\text{m}/\text{min}$ . After deposition, the sample sat at  $\sim 5.3$  K for 23 h, and then we began raising  $T$  at  $\sim 0.5$  K/20 min. (10-06-0296-0312pb01)

temperature is due primarily to the complicated time dependence at constant temperature. The lowest value for  $R_{\text{fcc/hcp}}$  is the steady state value. The plot is approximately linear from 6 K to 11 K. For  $D_2$  deposited between 5.1 K and 5.5 K and held at constant temperature for about two days, there is no change in  $R_{\text{fcc/hcp}}$ . Thus, after relaxation,  $R_{\text{fcc/hcp}}$  is roughly constant at constant temperature and decreases with increasing temperature.

The Raman spectrum of  $D_2$  deposited at 3.5 K [see Fig. 1(d)] behaves differently. As  $T$  is increased from  $T_d$  to 7 K, the two overlapping lines in the right branch separated slightly, but the general structure still consisted of two main branches. Upon increasing  $T$  to  $\sim 10$  K, the structure transformed into a well resolved triplet, similar to that shown in Fig. 1(f), within  $\sim 10$  min.

## Discussion of Raman Data

In Table 1 we list the theoretical and measured line positions for the Raman multiplet for both hcp and fcc crystal structures. We calculate the theoretical values from Van Kranendonk.<sup>7</sup> The measured values are from the present work and Bhatnagar et al.<sup>14</sup> The calculated

TABLE 1. Calculated and measured  $J=0 \geq 2$  Raman line positions (in  $\text{cm}^{-1}$ ) for  $H_2$  and  $D_2$  in hcp and fcc phases.

	$H_2$			$D_2$		
	Calculated	Ref. 15	Fig. 1	Calculated	Ref. 15	Fig. 1
hcp						
$m_j=2$	354.5	353.85	354	179.6	179.4	179
$m_j=1$	352.0	351.84	352	176.5	176.8	177
$m_j=0$	357.0	355.83	356	182.7	182.0	182
fcc						
$E_1$	349.6		350	173.6		175
$E_2$	356.9		356	182.6		182

values for the hcp lattice are close to the measured values. The calculated low-energy line of an fcc structure is at the same position as the low-energy line of the quadruplet spectra in Fig. 1(b) and 1(e). The calculated high-energy line of the fcc lattice would be unresolved from the high-energy hcp line given our resolution. Because of the low-energy line position in the quadruplet spectrum and the change in intensity of the high-energy line upon warming to  $T=0.5T_{\text{tp}}$ , we interpret the quadruplet spectrum to be the signature of a mixed hcp and fcc lattice. Thus, the narrow-line resolved spectra of Fig. 1(b) and 1(e) reflect the presence of both hcp and fcc crystallites.

The relative  $m_j=1, 2, 0$  intensity ratios for Fig. 1(a), 1(c), and 1(f) are 0.33:1:0.15, 0.55:1:0.21, and 0.64:1:0.34. The relative  $m_j$  intensities depend on crystal orientation with respect to the incident and scattered electric field

polarizations.<sup>7,15</sup> Assuming the incident light is collimated, a powder average of hcp crystallites yields 1:1:0.5, and a crystal with its *c* axis perpendicular to the substrate yields 0:1:0. Thus, there is a preferential *c*-axis alignment perpendicular to the substrate. Although a preferential growth along the *c* axis has been observed near the triple point, it is unclear why these small crystals would grow in a preferred direction or transform from fcc to hcp in a preferred orientation.

As  $T_d$  decreases in the range  $0.2 < T_d/T_{tp} < 0.3$ , the intensities of the low- and high-energy peaks increase relative to the two central peaks. After deposition, as  $T$  is increased towards  $0.5 T_{tp}$ , the low- and high-energy peaks decrease. This is expected if an fcc component occurs at  $T_d/T_{tp} < 0.3$  and increases with decreasing  $T_d$ . Thus, the ratio  $R_{fcc/hcp}$  is a relative measure of fcc to hcp structure in the sample. The irreversible decrease in  $R_{fcc/hcp}$  with increasing temperature suggests that the fcc component, once formed, is metastable at  $T < 0.5 T_{tp}$ . The equilibration of  $R_{fcc/hcp}$  after each temperature increase suggests that the fcc phase is separated from the lower-energy hcp phase by many different barrier energies. At constant  $T_d$ , we also see a slight increase in the fcc component with decreasing  $R$ . This implies that the fcc component may be found at  $T_d/T_{tp} > 0.3$  if we deposited at lower  $R$ . This effect may be due to sample heating.

Relative to their triple points, the temperature at which the mixed fcc + hcp structure is formed is lower in  $H_2$  (~4 K) than in  $D_2$  (~6 K). Also, the mixed phase transforms to pure hcp at a relatively lower temperature in  $H_2$  (~5.5 K) than in  $D_2$  (~10.5 K). Thus the fcc phase is less stable in  $H_2$  than in  $D_2$ . If the fcc phase is metastable and separated from the hcp phase by a spectrum of energy barriers, and if tunneling is a dominant mechanism for molecular motion at these low temperatures, then  $H_2$  would be able to cross the energy barriers to reach the lower-energy hcp phase more rapidly than  $D_2$ . Although tunneling diffusion has been observed for hydrogen atoms in solid hydrogen,<sup>16</sup> tunneling of molecules in solid hydrogen has not been clearly observed.<sup>17</sup>

The unresolved lineshape of Fig. 1(d) is significantly different than the other narrow line spectra in Fig. 1. This broad lineshape indicates that the lattice structure of samples deposited at  $T_d < 0.2 T_{tp}$  have less symmetry than pure hcp or fcc. The broad lineshape may result from a randomly stacked close-packed lattice or very small crystallites, but probably not an amorphous structure, which would give rise to a single broad line similar to that of the liquid phase.

## Crystal Morphology

Figure 3(a) and 3(b) show shadowgraph images of  $H_2$  crystallites deposited at  $R = 40 \mu\text{m}/\text{min}$  and  $T_d = 3.6 \text{ K}$

and 7.0 K. These and similar experiments qualitatively show that the average crystal size decreases rapidly with decreasing temperature and increasing deposition rate between  $3.6 < T_d < 11 \text{ K}$  and  $0.1 < R (\mu\text{m}/\text{min}) < 40$ . Figure 4 shows the change in the average crystal diam vs different  $T_d$ . The smallest crystal diam is at the limit of our optical resolution ( $\sim 3 \mu\text{m}$ ) and is thus a very rough estimate.<sup>18</sup>

Since the deposition temperatures used here are below the roughening transition temperatures for the low-energy crystal facets,<sup>19</sup> the lowest-free-energy configuration is in the form of faceted crystallites. The appearance of smooth rounded crystallites as in Fig. 3(b) implies that the crystal morphology is nonequilibrium and is determined by kinetics. To qualitatively understand the dependence of crystal size on temperature and deposition rate, we assume that the temperature controls the rate at which molecules relax from a high-energy to low-energy configuration. We expect the

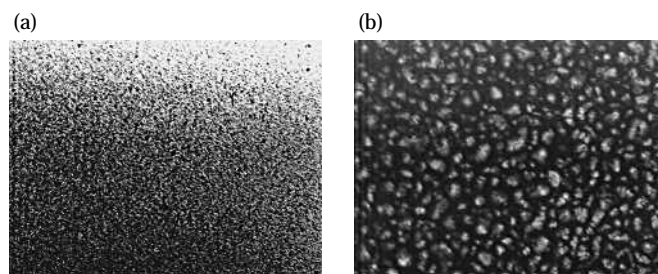


FIGURE 3. Shadowgraph images of  $H_2$  deposited at  $40 \mu\text{m}/\text{min}$  and (a) 3.6 K and (b) 7.0 K. The horizontal field of view is 1.7 mm. (10-06-0296-0312pb01)

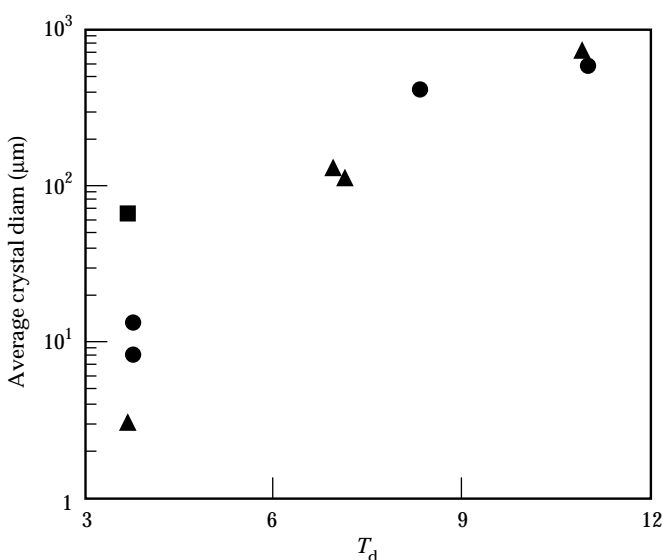


FIGURE 4. Average crystallite diam vs  $T_d$  for  $H_2$  deposited at  $0.2 \mu\text{m}/\text{min}$  (squares),  $2 \mu\text{m}/\text{min}$  (circles), and  $40 \mu\text{m}/\text{min}$  (triangles). (10-06-0296-0312pb01)

lowest-energy site to be that with the maximum number of neighboring bonds, such as a step edge of a crystal. As the temperature decreases or the deposition rate increases, there is less chance of finding a low-energy site before the next layer of material covers the substrate.

## Summary

In summary, using Raman spectroscopy we find that  $J=0$   $D_2$  or  $J=0$   $H_2$  forms a mixed fcc/hcp structure when deposited at  $0.2 < T_d/T_{tp} < 0.3$ . The fcc phase is less stable in  $H_2$  than  $D_2$ . This fcc component transforms continuously and irreversibly to hcp upon increasing the temperature through  $0.5 T_{tp}$ , suggesting that the fcc phase is separated from the lower-energy hcp phase by a spectrum of barrier energies. As  $T_d$  decreases below  $\sim 0.2 T_{tp}$ , the lattice structure has less symmetry than fcc or hcp and possibly resembles a randomly stacked close-packed phase. Finally, the crystallite size decreases with decreasing  $T_d$  from millimeter scale at a few degrees below  $T_{tp}$  to micrometer scale at  $\sim 0.3 T_{tp}$ .

The metastable hydrogen structure described here may elucidate several recent experiments. D atoms in solid deuterium deposited from the gas phase at  $\sim 3$  K have a significantly different activation energy than expected for the equilibrium hcp structure.<sup>17,20</sup> Also, surface-state electron mobility<sup>21</sup> shows an increased conductivity after annealing vapor-deposited films. These observations can be at least qualitatively explained by the metastable structures described here and those that may be found at lower deposition temperatures.

## Notes and References

1. J. J. Sanchez et al. *ICF Quarterly Report* 4(3), 117, Lawrence Livermore National Laboratory, Livermore, CA, UCRL-LR-105821-94-3 (1994).
2. A. J. Martin, R. J. Simms, and R. B. Jacobs, *J. Vac. Sci. Technol. A* 6(3), 1885 (1988); J. K. Hoffer and L. R. Foreman, *Phys. Rev. Lett.* 60, 1310 (1988); T. P. Bernat, E. R. Mapoles, and J. J. Sanchez, *ICF Quarterly Report* 1(2), 57, Lawrence Livermore National Laboratory, Livermore, CA, UCRL-LR-105821-91-2 (1991); G. W. Collins et al., *ICF Quarterly Report* 3(2), 81, Lawrence Livermore National Laboratory, Livermore, CA, UCRL-LR-105821-93-2 (1993).
3. I. V. Aleksandrova, E. R. Koresheva, and I. E. Osipov, Russian Academy of Sciences, P. N. Lebedev Physical Institute, Report No. 57, Moscow (1992).
4. Isaac F. Silvera, *Rev. Mod. Phys.* 52, 80 (1980).
5. Isaac F. Silvera, *Rev. Mod. Phys.* 52, 393 (1980).
6. P. C. Souers, *Hydrogen Properties for Fusion Energy* (University of California, Berkeley, 1986), Ch. 6.
7. Jan Van Kranendonk, *Solid Hydrogen* (Plenum Press, New York, 1983), p. 226.
8. K. F. Niebles and J. A. Venables in *Rare Gas Solids*, M. L. Klein and J. A. Venables, Eds. (Academic Press, New York, 1976), vol. 1, Ch. 9.
9. R. L. Mills, J. L. Yarnell, and A. F. Schuch, *Proceedings of the Low Temperature Physics Conference 13*, Boulder (Plenum, NY) vol. II, p. 202; O. Bostanjoglo and R. Kleinschmidt, *J. Chem. Phys.* 46, 2004 (1967); A. E. Curzon and A. J. Mascall, *Brit. J. Appl. Phys.* 16, 1301 (1965); C. S. Barrett, L. Meyer, and J. Wasserman, *J. Chem. Phys.* 45, 834 (1966).
10. The substrate was an amorphous or nanocrystalline film of  $MgF_2$  vapor deposited onto a sapphire window that was cleaved normal to the c axis.
11. I. F. Silvera and R. J. Wijngaarden, *Phys. Rev. Lett.* 47, 39 (1981). R. J. Wijngaarden, Ph.D. thesis, Harvard University, University Microfilms, Ann Arbor, MI, 1982.
12. S. C. Durana and J. P. McTague, *Phys. Rev. Lett.* 31, 990 (1973).
13. Isaac F. Silvera, *Rev. Mod. Phys.* 52, 49 (1980).
14. S. S. Bhatnagar, E. J. Allin, and H. L. Welsh, *Can. J. Phys.* 40, 9 (1962).
15. J. P. McTague, I. F. Silvera, and W. N. Hardy, *Proceedings of the 7th AIRAPT Conf. on Light Scattering in Solids*, Paris, France, 1971 (Flammarion Sciences, Paris) p. 456.
16. G. W. Collins et al., *Phys. Rev. B* 45, 549 (1992); A. S. Iskovskikh et al., *Sov. Phys. JETP* 64, 1085 (1986).
17. J. R. Gaines, P. A. Fedders, G. W. Collins, J. D. Sater, and P. C. Souers, *Phys. Rev. B* 52, 7243 (1995).
18. Crystals left at constant temperature, even near 3.5 K, appeared to increase with time, although we did not study this phenomenon in detail. The crystal size for  $T > 0.7$ ,  $T_{tp}$  also depends on layer thickness. For the data in Fig. 4, the layers are about 50  $\mu m$  thick. Layers thinner than 10 to 20  $\mu m$  have smaller crystals.
19. G. W. Collins, E. R. Mapoles, W. Unites, T. P. Bernat, "Roughening Transition in Solid Deuterium," Lawrence Livermore National Laboratory, Livermore, CA, UCRL-JC-117390 (1994).
20. A. V. Ivliev et al., *JETP Lett.* 38, 379 (1983); E. B. Gordon et al., *JETP Lett.* 37, 282 (1983).
21. M. A. Paalanen and Y. Iye, *Surface Science*, 170, 80 (1986); K. Kono, U. Albrecht, and P. Leiderer, *J. Low Temp. Physics*, 82, 279 (1991).